Journal of Solid State Chemistry **148,** 316–324 (1999)
Article ID jssc.1999.8453, available online at http://www.idealibrary.com on IDEAL®

Thermal Analysis and X-Ray Diffraction Study on $LiKSO_4$: A New Phase Transition

Xavier Solans,* M. Teresa Calvet,* M. Luisa Martínez-Sarrión,† Lourdes Mestres,† Aniss Bakkali,† Eduardo Bocanegra,‡ Jorge Mata,* and Marta Herraiz†

*Departamento de Cristal.lografia, Mineralogia, i Dipòsits Minerals, Universitat de Barcelona, E-08028-Barcelona, Spain; †Departmento de Química Inorgànica, Universitat de Barcelona, E-08028-Barcelona, Spain; and ‡Departamento de Física Aplicada II, Universidad del Pais Vasco, E-48080-Bilbao, Spain

Received April 19, 1999; in revised form July 13, 1999; accepted July 22, 1999

Results of a detailed X-ray diffraction and thermal analysis study of the structural phase transitions in $LiKSO_4$ carried out in the temperature range 123–1000 K are presented. The study indicates five phase transitions in the temperature range studied at 937, 707, 226 (268), 200 (251), and 186 (190) K (values in parentheses are for a warming process). The transition at 226 (268) K is reported for the first time. The different phases (from high to low temperature) show the space groups $P6_3/mmc$, $P2_1cn$, $P6_3$, $P6_3mc$, $P3_1c$, and $Cmc2_1$. The working conditions allowed us to obtain the different phases without twin crystals and without mixtures of several phases. We were thus able to determine the crystal structures of the different phases with more accuracy. The transitions at high temperature produce large variations in the crystal structure and the enthalpy of process is high, while at low temperature, as the structure is more compact, an activation energy is necessary, and the transitions show a thermal hysteresis, while the structural variation is as small as the enthalpy of the process. © 1999 Academic Press

INTRODUCTION

In recent years, a great number of studies have been reported on the physical properties of, and the phase transitions in, lithium potassium sulfate, $LiKSO_4$. The interest of this compound is due to its pyroelectric, superionic conductivity, ferroelastic and ferroelectric properties, and the discovery of several phase transitions in the temperature range 10 to 950 K. These phase transitions have been studied using a variety of techniques: thermal expansion (1), thermal analysis (2, 3), laser–Raman spectroscopy (4–7), NMR (8), ESR (9–14), electrical and optical studies (15–23), and diffraction (24–31). In general, the conclusions drawn by various authors are contradictory. The phase transitions of $LiKSO_4$ in the range 150 to 1000 K are summarized in Table 1.

In our literature revision, we have observed that some authors worked with twinned crystals, while other authors did not test the quality of crystal and the heating and cooling rates and the sample masses were not specified by them. In order to elucidate and to characterize the phase transition of the title compound, a thermal and X-ray diffraction study has been carried out.

EXPERIMENTAL SECTION

Synthesis

The lithium potassium sulfate was obtained via the reaction of K_2SO_4 with $Li_2SO_4H_2O$ in aqueous solution. The molar ratio between the potassium and lithium sulfates was 1:1.5. The obtained compound was analyzed by ICP (induced condensed plasma) with a Jobin–Yvon analyzer. Crystals were obtained by slow evaporation at 313 K.

Thermal Analysis

The thermal analysis for the temperature range 298–975 K was carried out in a differential thermal analysis (DTA) and thermogravimetry (TG) Netzsch 409. The warming rate was 10 K/min., the weight of the sample, was 101.5 mg, and the reference material was alumina. The sample did not lose weight throughout the process.

The thermal analysis for the temperature range 103–473 K was carried out in a differential scanning calorimeter (DSC) Perkin–Elmer DSC7. The weight of sample was 38.9 mg. The experiment was a cooling process followed by a warming process between the mentioned temperatures with the same cooling and warming rate (10 K/min). The phase transitions and enthalpies of the process are given in Table 2. As a new phase transition was observed at 250 K (Fig. 1), a warming process for the temperature range 200–293 K was carried out at different warming rates (5 and 2 K/min).

0022-4596/99 $30.00

TABLE 1
Phase Transitions of $LiKSO_4$ in the Range 150–1000 K, According to the References

Phase I:	Space groups: $Cmc2_1$, $P6_3$, Cc, $P6_3mc$	
	Physical prop.: ferroelastic, ferroelectric	
Transition I:	Temperature: 178–203 K	Thermal hysteresis: 0–32 K
Phase II:	Space groups: Incomensurate, $P3_1c$, $P6_3mc$	
	Physical prop.: ferroelectric, paraelastic	
Transition II:	Temperature: 200–210 K (cooling) 248–265 (heating)	Thermal hysteresis: 35–55 K
Phase IV:	Space groups: $P6_3$, $P2_1$	
	Physical prop.: paraelectric	
Transition IV:	Temperature: 708 K	Thermal hysteresis: 0 K
Phase V:	Space groups: $P2_1cn$, Incomensurate	
Transition V:	Temperature 941 K	Thermal hysteresis: 0 K
Phase VI:	Space groups: $P6_3mc$, $P6_3/mmc$	
(989 K pass to melt)		

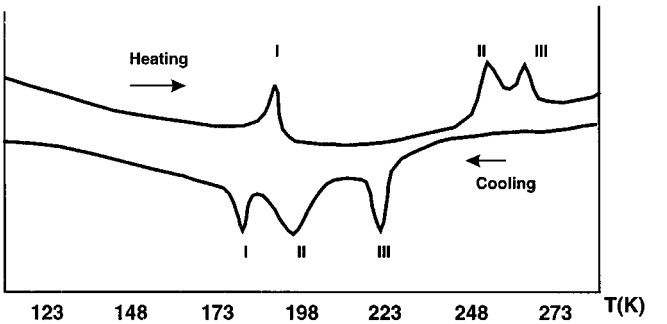

FIG. 1. The thermal analysis data of the low temperature phase transitions for the warming and cooling process.

X-Ray Powder Diffraction

Powder diffraction data in the range 298–968 K were collected using the Bragg–Brentano geometry with a Siemens D500 automated diffractometer, using Cu$K\alpha$ radiation and a secondary monochromator. The experiment was a warming process from 298 to 968 K, followed by a cooling process between the same temperatures with the same sample. The cooling and warming rates were 10 K/min, and the sample was left for 10 min at the measuring temperature in order to stabilize the equipment and the sample. Measurements were taken at 298, 473, 673–718 (every 5 K), 873, and 923–953 K (every 5 K) and at the same temperatures in the cooling process. The step size was 0.025°, the time of step 10 sec, and the 2θ range was 16–120°.

Powder diffraction data in the 163–298 K range were collected using Debye–Sherrer geometry, a 120° arch detector INEL, and the sample in a rotating capillary to diminish preferred orientation. The radiation was Cu$K\alpha$, using a primary planar quartz monochromator. The time of exposure was defined giving a minimum count for the highest reflection (about 1 h). All processes were followed with the same sample, first a cooling process with a cooling rate of 10 K/min, after which the sample was left for 10 min at the measuring temperature in order to stabilize the sample and the equipment, and a warming process at the same conditions and temperatures. The measurements were taken at 163–208 (every 5 K), 223, and 243–298 (every 5 K). Cell parameters (Fig. 2) from powder diffraction were determined using the TREOR (32) computer program and refined with the CELREF computer program (33).

TABLE 2
Onset Temperatures (K) and Enthalpies of the Phase Transitions Obtained from Thermal Analysis

Phase transition	T (H)	T (C)	ΔH
I	190	186	46 J mol^{-1}
II	251	200	33 J mol^{-1}
III	268	226	9 J mol^{-1}
IV	707	707	5 kJ mol^{-1}
V	937	937	1 kJ mol^{-1}

Note. H, heating, C, cooling.

X-Ray Structure Determination

A similar method was followed in all single-crystal structure determinations, using the same crystal. The intensities were measured at 298, 233, 189, 123, and 260 K. All phases were measured after cooling, with the exception of phase III (the new phase) which was measured after warming. Diffraction data were collected on an Enraf–Nonius CAD4 automated diffractometer equipped with a graphite monochromator. The ω–θ scan technique was used to record the intensities. Scan widths were calculated as $A + B \tan\theta$, where A is estimated from the mosaicity of the crystal and B allows for the increase in peak width due to Mo$K\alpha_1$–$K\alpha_2$ splitting.

Details of the structure determination are listed in Table 3. The unit-cell parameters were obtained by a least-squares fit to the automatically centered settings from 25 reflections ($12° < 2\theta < 21°$). The intensities from three control reflections for each measurement showed no significant fluctuation during the data collection.

The structures were solved by Patterson synthesis, using SHELXS-86 computer program (34) and refined by the full-matrix least-squares method, using the SHELXL-93 computer program (35). The function minimized was $w||F_o|^2-|F_c|^2|^2$, where the weighting scheme was $w = [\sigma^2(I) + (k_1P)^2 + k_2P]^{-1}$ and $P = (|F_o|^2 + 2\ |F_c|^2)/3$. The

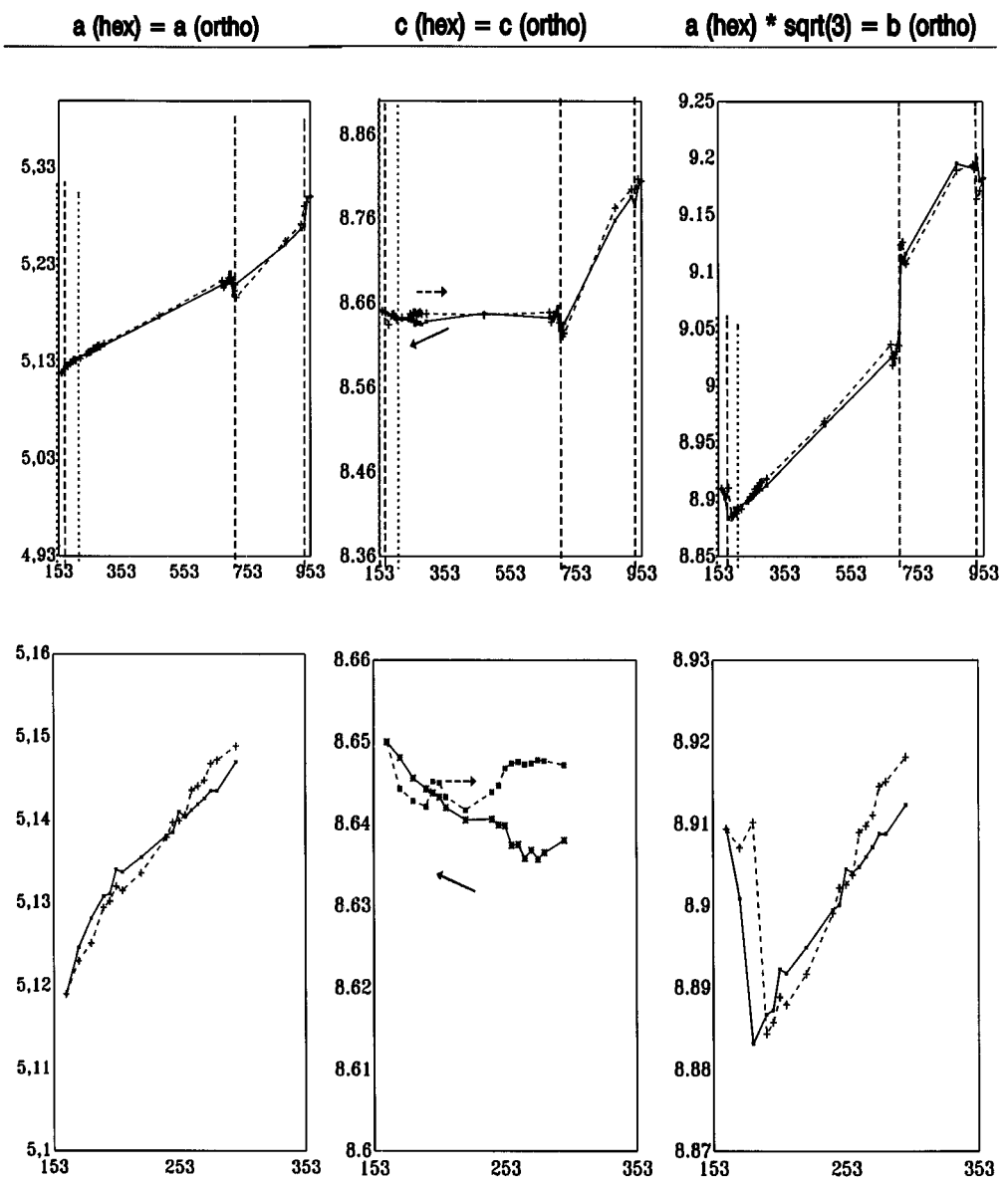

FIG. 2. Cell-parameters versus temperature, obtained from X-ray diffraction on powder samples. In the bottom the sector at low temperature is shown with a more appropriate scale.

values of k_1 and k_2 were also refined. The chirality of the structure was defined from the Flack coefficient (36).

Structures at 773 and 973 K were determined from a powder sample. Diffraction data were recorded with the Siemens D-500 diffractometer. The step of scan was 0.025° and the time of the step was 10 s. The structures were solved by direct methods using the SIRPOW computer program (37) and refined using the FULLPROF computer program (38). The Li position in both structures was constrained to be in the center of its tetrahedron, O positions in the structure at 773 K were constrained to have the same S–O bond length. The intensity statistic at 773 K shows that the space group is $P2_1cn$, while that at 973 K is $P6_3/mmc$, which was confirmed with the refinement. Details of the refinement are given in Table 4. The chirality of structure at 773 K was defined from the results at low temperature. Final atomic coordinates are given in Table 5. Figures 3 and 4 shows two projections of the cell content.

RESULTS AND DISCUSSION

The results of DTA, DSC, and TG analyses (Table 2) show that the $LiKSO_4$ underwent five phase transitions in the temperature range studied (103–975 K). Four of them

TABLE 3
Crystal Data and Structure Refinement for Structure Determined by Single-Crystal Diffractometry

	For all structures				
Empirical formula	$KLiSO_4$				
Formula weight	142.10				
Wavelength (Å)	0.71069				
Crystal size (mm)	$0.3 \times 0.2 \times 0.2$				
Theta range for data collection	4.58 to 29.89°				
Refinement method	Full-matrix least-squares on F^2				
Temperature (K)	298(1)	233(1)	189(1)	260(1)	123(1)
Crystal system	Hexagonal	Hexagonal	Trigonal	Hexagonal	Orthorhombic
Space group	$P6_3$	$P6_3$	$P3_1c$	$P6_3mc$	$Cmc2_1$
a (Å)	5.1421(11)	5.1341(12)	5.117(2)	5.123(2)	5.114(2)
b (Å)	5.1421(11)	5.1341(12)	5.117(2)	5.123(2)	8.857(3)
c (Å)	8.634((2)	8.638(3)	8.638(6)	8.639(3)	8.630(3)
Volume (Å^3)	197.71(8)	197.18(9)	195.9(2)	196.38(11)	390.9(2)
Z	2	2	2	2	4
Dx (Mg/m^3)	2.387	2.393	2.409	2.403	2.415
μ (mm^{-1})	1.734	1.739	1.750	1.746	1.754
$F(000)$	140	140	140	140	280
Index ranges	$-6 \le h \le 7$ $-6 \le k \le 7$ $0 \le l \le 12$	$-6 \le h \le 7$ $-6 \le k \le 7$ $0 \le l \le 12$	$-6 \le h \le 7$ $-6 \le k \le 7$ $0 \le l \le 12$	$-6 \le h \le 7$ $-6 \le k \le 7$ $0 \le l \le 12$	$0 \le h \le 7$ $0 \le k \le 12$ $0 \le l \le 12$
Reflections collected	660	660	660	660	310
Independent refl.	205	206	205	136	310
R (int)	0.012	0.010	0.045	0.034	–
Data/parameters	200/23	199/23	203/23	133/23	310/53
S (F^2)	0.862	0.971	1.040	1.034	1.149
Final $R(F)$	0.029	0.025	0.073	0.051	0.054
Final w$R(F^2)$	0.071	0.079	0.188	0.135	0.128
Flack parameter	0.2(2)	0.10(11)	0.9(4)	0.2(4)	0.1(3)
Extinction coeff.	3.4(2)	0.69(3)	0.00(5)	0.56(12)	0.00(1)
Largest diff. syn. peak (e.Å^{-3})	0.323	0.309	0.509	0.518	0.497
hole (e.Å^{-3})	−0.433	−0.345	−0.577	−0.331	−0.419

had been described previously. The transitions at 226 (in the cooling process) and 268 K (in the warming process) are reported for the first time. The results obtained for transitions II and III at different warming rates are: rate 10 K/min, transition temperatures 251 and 268 K; 5 K/min, 250 and 267 K; and 2 K/min, 251 and 267 K. This shows that the thermal effect is independent of kinetics, as is the existence of the phase transition. The ΔH of the IV phase transition is close to the value obtained for the transition of K_2BeF_4 (39) at 913 K (5 kJ mol^{-1}) and higher than those obtained for $(NH_4)_2SO_4$ (40) at 223 K (3.9 kJ mol^{-1}). The ΔH of the V transition is close to the value obtained (1.3 kJ/mol) for the transition of $(NH_4)_2BeF_4$ at 176 K (40). The ΔH of the transitions at low temperature are higher than those obtained for the transition at 93 K of K_2SeO_4 (41) (2 J/mol). The transitions at low temperature show thermal hysteresis.

Cell parameters were refined using all identified maxima in the powder patterns. Peaks of two phases are observed from 928 to 948 K. The space groups of different phases according to systematic absences are $Cmc2_1$ for phase I, $P3_1c$ for phase II, $P6_3mc$ or $P6_3/mmc$ for phase III, $P6_3$ for phase IV, $P2_1cn$ for phase V, and $P6_3mc$ or $P6_3mmc$ for phase VI. Phase transition III is not clear from powder diffraction, but an anomalous behavior in the cell parameters (Fig. 2) and the modification of the intensity of some reflections were observed. The highest variation in cell parameters was observed in transitions I and IV with a major increase of the b_{ortho} cell parameter.

We have solved the crystal structures at 298, 260, 233, 189, and 123 K without using a twin crystal. This has not been made and reported previously. The crystal structure at 189 K was poorly resolved, which may be because the measuring temperature is close to a transition temperature in this crystal. This was not due to the quality of the crystal, because in the following measurements the results were correct. The space groups of the $LiKSO_4$ phases are $P3_1c$ for phase II, $P6_3mc$ for phase III, and $P6_3$ for phase IV.

The crystal structure at 973 K (phase VI) can be described as a hexagonal close packing of sulfate tetrahedra, with the

TABLE 4
Crystal Data and Structure Refinement for Structures Determined by Powder Diffractometry

Empirical formula	$LiKSO_4$	$LiKSO_4$
Formula weight	142.10	142.10
Temperature (K)	773	973
Crystal system	orthorhombic	hexagonal
Space group	$P2_1cn$	$P6_3/mmc$
a (Å)	5.2150(3)	5.2997(3)
b (Å)	9.1321	5.2997(3)
c (Å)	8.6652(4)	8.8021(6)
Volume (Å^3)	412.7(2)	214.10(4)
Z	4	2
ρ(calculated) (Mg/m^3)	2.286	2.204
μ (mm^{-1})	1.624	1.565
$F(000)$	280	140
θ range (•)	15–100	15–100
No. of data	3401	3389
Refl. collected	484	116
Refined parameters	30	20
R_{wp}	7.4	6.11
R_B	12.9	9.1
S	5.3	8.47
DWD	1.91	1.90

Note. $R_{wp} = 100 \times \{\sum w_i(y_i - y_{0i})^2/\sum w_i y_i^2\}^{1/2}$. $R_B = 100 \sum \bullet I_o - I_c \bullet / \sum I_o$. S = Goodness of fit = $R_{wp}/R_{expected}$. DWD = weighted Durbin–Watson statistic D.

K ions occupying the octahedral sites (every K ion is surrounded by six sulfate ions) and the Li ions occupying the tetrahedral sites. This produces a framework of corner-shared LiO_4 and SO_4 tetrahedra with K filling the cavities within the framework. The K ion displays a tricapped trigonal prism coordination with respect to oxygen atoms.

The shrinking of the K^+ cavity produces phase V. The sulfate ion rotates 20° around the c-axis and 25° around an axis perpendicular to it, which leads to the structure at 773 K. These rotations produce a large cavity for the Li^+ ion. This fact was suggested by Pimenta *et al.* (19) from infrared reflectivity. The sulfate ion rotates $-38°$ around the c-axis and $-25°$ around an axis perpendicular to it, which leads to the structure at 298 K (phase IV). In this structure the S and Li tetrahedra are distorted in such a way that the O(2)–X–O(2) angle is larger than the O(2)–X–O(1) angle.

Phase IV was measured at two different temperatures (298 and 233 K). The differences between these two structures are the rotation of $-2°$ of the sulfate ion when the temperature falls and the shortening of K–O(2) length (from 2.836(3) to 2.826(2) Å). The structure at 189 K (phase II) is a reorganization of the tetrahedral framework of the structure at 298 K. The sulfate ion rotates 56° around the c-axis, which reduces the K–O(2) stress. The structure at 260 K (phase III) is intermediate between those of phases II and IV and it is the typical twin phase shown by compounds with a high number of phase transitions. This suggests that phase III would not be detected if the conditions of analysis were more extreme than those reported here. The last phase, at 123 K, is a new disordered structure, where the sulfate ion rotates 4° or $-57°$ around the c-axis, depending of the assumed disorder position.

We have studied the stability of the structure from the bond-valence model and the distortion theorem described by Brown (42). At 973 K the K^+ ion occupies a large cavity which produces the instability of the structure. At 773 K the

TABLE 5
Atomic Coordinates ($\times 10^4$ .S,O, and Li atoms at 973 and 773 K$\times 10^3$)

		x	y	z
973 K	S	667	333	250
	K	0	0	0
	Li	667	333	615(8)
	O(1)	667	333	82(4)
	O(2)	515(8)	1030(8)	305(4)
773 K	S	707(6)	80(2)	777(1)
	K	2357	2031(8)	4956(10)
	Li	707(31)	387(10)	679(8)
	O(1)	435(7)	52(4)	745(4)
	O(2)	849(8)	−58(3)	773(4)
	O(3)	734(8)	147(2)	930(2)
	O(4)	810(7)	179(4)	660(3)
298 K	S	3333	6667	9007(2)
	K	10000	10000	11938(1)
	Li	3333	6667	5134(12)
	O(1)	3333	6667	7310(7)
	O(2)	5979(5)	9425(5)	9538(4)
233 K	S	3333	6667	9003(1)
	K	10000	10000	11939(1)
	Li	3333	6667	5134(9)
	O(1)	3333	6667	7321(4)
	O(2)	5991(4)	9422(4)	9546(3)
189 K	S	3333	6667	8863(3)
	K	10000	0	11831(3)
	Li	3333	6667	5113(26)
	O(1)	3333	6667	7300(36)
	O(2)	3567(26)	9495(48)	9246(14)
260 K	S	3333	6667	8873(3)
	K	10000	0	11815(3)
	Li	3333	6667	5008(27)
	O(1)	3333	6667	7167(14)
	O(2)	6014(21)	9447(20)	9419(10)
123 K	S	0	1667(2)	2375(3)
	K	0	4994(2)	315(2)
	O(1)	0	1579(11)	674(11)
	O(2)	−2838(26)	1726(11)	2897(16)
	O(3)	1476(30)	3064(13)	2848(18)
	O(4)	−1307(21)	332(10)	2982(13)
	Li	0	1870(23)	−1484(24)

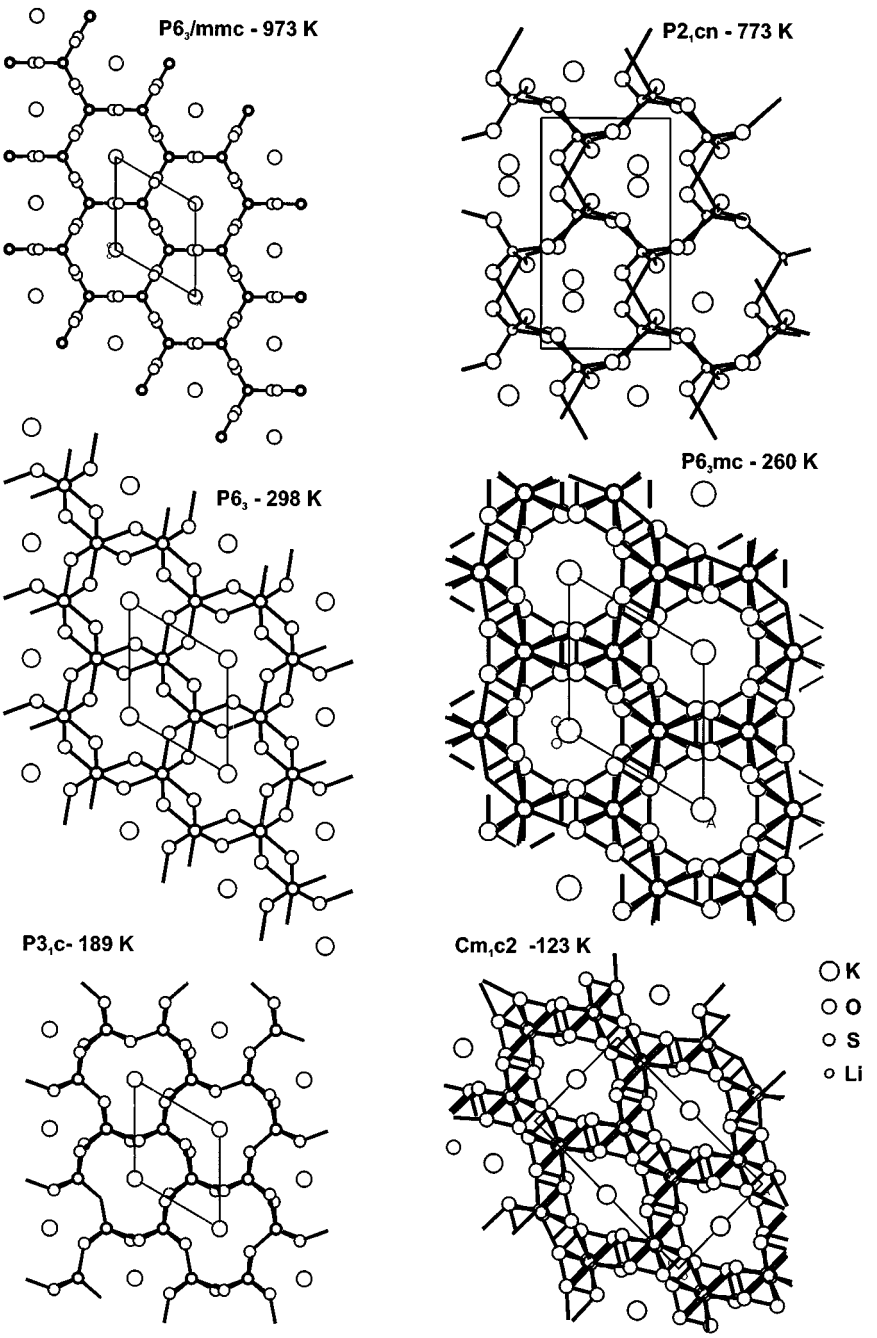

FIG. 3. Unit cell content of the different phases of $LiKSO_4$ viewed down the *c*-axis.

stress of the structure is in the K–O(4) bond, while the Li^+ ion occupies a larger cavity (sum of the bond valence 1.02 for K and 0.86 for Li ions). From 298 to 123 K the site driving the instability is the K ion which occupies the more asymmetric cavity (see Table 6).

It is important to note that the two disordered structures (phases III and I) have an average symmetry $P6_3mc$ and $Cmc2_1$. The local symmetry of these two phase is $P6_3$ and Cc, respectively, which may explain why the first was not observed and why the second gives conflicting results when the spectroscopic technique was used.

CONCLUSIONS

We have structurally characterized the six phases of $LiKSO_4$ in the temperature range 150–1000 K. The

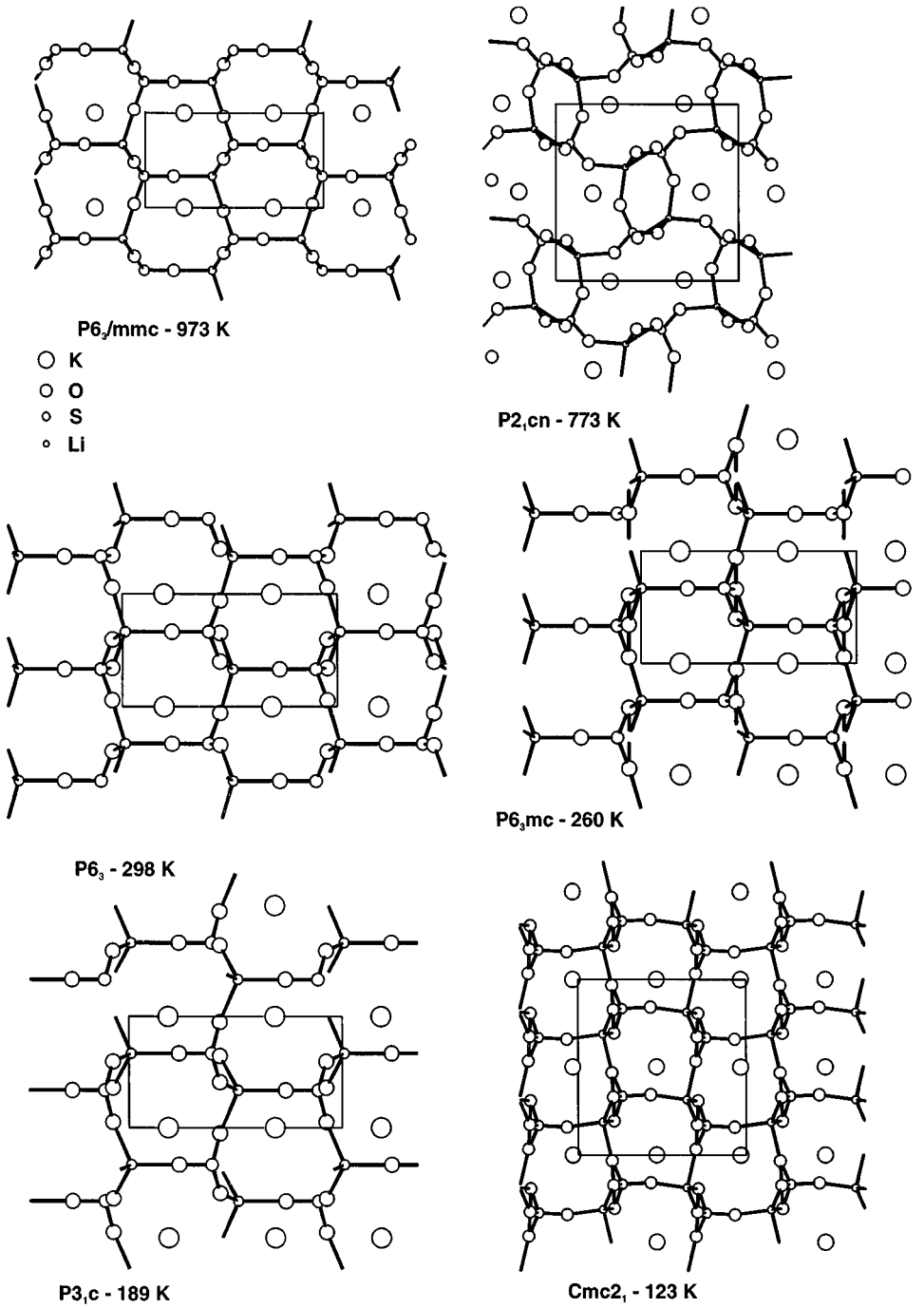

FIG. 4. Unit cell content of the different phases viewed parallel to the (010) plane.

working conditions allowed us to obtain the different phases without twin crystals and without mixtures of several phases; this has led to determination of the crystal structures of the different phases with greater accuracy. The framework of corner-shared LiO_4 and SO_4 tetrahedra is relatively flexible, shown by the large number of phases. The transition between phases, V and VI is order–disorder or displacive if phase VI is assumed to be multiple domains of $P6_3mc$ symmetry, giving an average structure of $P6_3/mmc$ symmetry. The second explanation would be to agree with those authors who assigned this space group to phase VI. The remaining transitions are displacive, except those to

TABLE 6
Bond Lengths [Å] and Angles [•]

	973 K	773 K	298 K	233 K	189 K	260 K	123 K
S–O	1.47(4) × 4	1.46(4) 1.46(4) 1.47(5) 1.47(2)	1.464(3) × 3 1.465(6) × 1	1.467(2) × 3 1.453(4) × 1	1.43(2) × 3 1.35(3) × 1	1.477(9) × 3 1.474(13) × 1	1.521(14) 1.470(10) 1.456(8) 1.506(14)
K–O	3.144(8) × 3 3.16(4) × 6	2.65(3) 2.74(3) 2.74(4) 2.99(4) 3.01(4) 3.02(3) 3.29(4) 3.32(4) 3.50(4)	2.836(3) × 3 2.965(3) × 3 2.9861(9) × 3	2.826(2) × 3 2.964(2) × 3 2.9824(8) × 3	2.867(14) × 3 2.976(12) × 3 2.982(5) × 3	2.821(8) × 3 2.955(9) × 3 2.974(2) × 3	2.923(12) × 1 2.810(12) × 1 2.934(5) × 1 2.776(10) × 2 2.839(14) × 2 2.876(14) × 2
Li–O	1.84(4) × 1 1.77(5) × 3	1.98(10) 1.99(16) 2.02(12) 2.18(17)	1.878(10) × 1 1.928(4) × 3	1.889(7) × 1 1.927(3) × 3	1.89(4) × 1 1.95(2) × 3	1.86(2) × 1 1.915(10) × 3	1.88(2) 1.75(2) 1.89(2) 2.11(2)
O–S–O	109.2(14) × 3 109.7(14) × 3	109(2) 109(3) 109(2) 110(2) 110(2) 110(3)	110.6(2) × 3 108.3(2) × 3	110.28(9) × 3 108.65(9) × 3	103.4(5) × 3 114.8(4) × 3	110.3(3) × 3 108.6(4) × 3	108.4(6) 109.9(7) 108.3(7) 111.0(6) 107.3(5) 111.7(8)

pass to phases III and I, where we did not elucidate the domain of each disordered site. However, the disordered phases are at low temperature, so thermodynamic reasons suggest that these phases have multiple domains of $P6_3$ and Cc symmetry and the phase transitions are also displacive. The conclusion of multiple domains for phase I agrees with the crystal optical studies of Kleemann, Schäfer, and Chaves (21) who observed the formation of domains for this phase.

The phase transitions at high temperature produce large variations in the crystal structure; the enthalpy of the process is high and the transitions do not shown thermal hysteresis. A hysteresis of 3 K was only observed at the phase transition IV by electrical conductivity measurements (19), but it is not observed by IR reflection spectra. Brillouin scattering (19), powder diffraction, thermal analysis (this work), or linear bi-refrigence (21). At low temperature, as the structure is more compact (the c-parameter remains practically constant, Fig. 2), an activation energy is necessary and the transitions show thermal hysteresis, while the structural variation is as small as the enthalpy of the process.

REFERENCES

1. D. P. Sharma, *Pramana*, **13,** 223 (1979).
2. I. M. Iskornev, I. N. Flerov, M. V. Gorev, L. A. Kot, and V. A. Grankina, *Soviet Phys.: Solid State* **26,** 1926 (1984).
3. L. Abello, K. Chhor, and C. Pommier, *J. Chem. Thermodynam.* **17,** 1023 (1985).
4. M. L. Bansal, S. K. Deb, A. P. Roy, and V. C. Sahni, *Solid State Commun.* **36,** 1047 (1980).
5. J. Mendes-Filho, J. E. Moreira, F. E. A. Melo, F. A. Germano, and A. S. B. Sombra, *Solid State Commun.* **60,** 189 (1986).
6. A. J. Oliveira, F. A. Germano, J. Mendes-Filho, F. E. A. Melo, and J. E. Moreira, *Phys. Rev. B* **38,** 12633 (1988).
7. F. Ganot, B. Kihal, R. Farhi, and P. Moch, *Jap. J. Appl. Phys.* **24,** 491 (1985).
8. B. Topic, U. Haeberlen and R. Blinc, *J. Phys. B-Condens. Matter* **70,** 95 (1988).
9. F. Holuj and M. Drozdowski, *Ferroelectrics* **36,** 379 (1981).
10. T. Shibata, R. Abe, and M. Fukui, *J. Phys. Soc. Japan* **55,** 2088 (1986).
11. J. T. Yu and S. Y. Chou, *J. Phys. Chem. Solids* **47,** 1171 (1986).
12. J. T. Yu, J. M. Kou, S. J. Huang, and L. S. Co, *J. Phys. Chem. Solids* **47,** 121 (1986).
13. K. Murthy, U. Ramesh, and S. V. Bhat, *J. Phys. Chem. Solids* **47,** 927 (1986).
14. K. Maezawa, T. Takeuchi, and K. Ohi, *J. Phys. Soc. Japan* **54,** 3106 (1985).
15. S. Fujimoto, N. Yasuda, H. Hibino, and P. S. Narayanan, *J. Phys. D: Appl. Phys.* **17,** L35 (1984).
16. B. Mroz, T. Krajewski, T. Breczewski, W. Chomka, and D. Sematowicz, *Ferroelectrics* **42,** 71 (1982).
17. T. Krajewski, T. Breczewski, M. Kassem, and B. Mroz, *Ferroelectrics* **55,** 143 (1984).
18. G. Sorge and H. Hempel, *Phys. Stat. Solidi A* **97,** 431 (1986).
19. M. A. Pimenta, P. Echegut, Y. Luspin, G. Hauret, F. Gervais, and P. Abèlard, *Phys. Rev. B* **39,** 3361 (1989).

20. T. Breczewski, T. Krajewski, and B. Mroz, *Ferroelectrics* **33,** 9 (1981).
21. W. Kleemann, F. J. Schäfer, and A. S. Chaves, *Solid State Commun.* **64,** 1001 (1987).
22. J. Ortega, T. Eyxebarría, and T. Breczewski, *J. Appl. Cryst*. **26,** 549 (1993).
23. K. Staduicka, A. M. Glazer, and S. Arzt, *J. Appl. Cryst*. **26,** 555 (1993).
24. P. E. Tomaszewski and K. Lukaszewicz, *Phase Transitions* **4,** 37 (1983).
25. R. H. Chen and R. T. Wu, *J. Phys. Condens. Matter* **1,** 6913 (1989).
26. S. Bhakay-Tamhane, A. Sequeira, and R. Chidambaram, *Acta Cryst*. *C* **40,** 1648 (1984).
27. S. Bhakay-Tamhane and A. Sequeira, *Ferroelectrics* **69,** 241 (1986).
28. A. M. Balagurov, B. Mroz, N. C. Popa, and B. N. Savenko, *Phys. Stat*. *Sol*., *A* **96,** 25 (1986).
29. S. Bhakay-Tamhane, A. Sequeira, and R. Chidambram, *Phase Transition* **35,** 75 (1991).
30. Y. Y. Li, *Solid State Commun.* **51,** 355 (1984).
31. H. Schulz, U. Zucker, and R. Frech, *Acta Cryst*., *B* **41,** 21 (1985).
32. P. E. Werner, "TREOR, Trial and error program for indexin of unknown powder patterns," University of Stockholm, Sweden, 1984.
33. J. Laugier and A. Filhol, "Programme CELREF, ILL," Grenoble, France, 1978.
34. G. M. Sheldrick, *Acta Cryst*. *A* **46,** 467 (1990).
35. G. M. Sheldrick, "SHELXL, A computer program for crystal structure determination." Univ. Göttingen, Germany, 1993.
36. H. D. Flack, *Acta Cryst*. *A* **39,** 867 (1983).
37. A. Altomare, G. Cascarano, C. Giacovazzo, A. Guagliardi, M. C. Burla, G. Polidori, and M. Camalli, "SIRPOW, Instituto di Ricerca per lo Svilupp di Metodologie Cristallografiche," Universita di Bari, Italy, 1992.
38. J. Rodríguez-Carvajal, "FULLPROF," Version 3.1c. Laboratoire Leon Brillouin, Paris, France, 1996.
39. X. Solans, C. González-Silgo, M. T. Calvet, C. Ruiz-Pérez, M. L. Martínez-Sarrión, and L. Mestres, *Phys. Rev. B* **57,** 5122 (1998).
40. S. Hoshino, K. Vedam, Y. Okaya, and R. Pepinsky, *Phys. Rev*. **112,** 405 (1958).
41. K. Aiki, K. Hukuda, H. Kaga, and T. Kobayashi, *J. Phys. Soc. Jpn.* **28,** 389 (1970).
42. I. D. Brown, *Acta Cryst*., *B* **48,** 553 (1992).